Predicting the breaking onset of surface water waves

Alexander Babanin,[1] Dmitry Chalikov,[2] Ian Young,[3] and Ivan Savelyev[4]

[1] Why do ocean waves break? Understanding this important and obvious property of the ocean surface has been elusive for decades. This paper investigates causes which lead deep-water two-dimensional initially monochromatic waves to break. Individual wave steepness is found to be the single parameter which determines whether the wave will break immediately, never break or take a finite number of wave lengths to break. The breaking will occur once the wave reaches the Stokes limiting steepness. The breaking probability and the location of breaking onset can be predicted, properties of incipient breakers measured. Potential applications to field conditions are discussed. **Citation:** Babanin, A., D. Chalikov, I. Young, and I. Savelyev (2007), Predicting the breaking onset of surface water waves, *Geophys. Res. Lett.*, *34*, L07605, doi:10.1029/2006GL029135.

1. Introduction

[2] One of the most elusive questions in fluid mechanics surrounds the mechanism responsible for the breaking of water waves. Wave breaking is ubiquitous on the ocean surface and is manifested by the appearance of sporadic white-caps. A full understanding of such wave breaking and an ability to predict its onset has been hindered by the strong nonlinearity of the process, together with its irregular and intermittent nature.

[3] Of the processes responsible for the evolution of wind-generated waves, breaking dissipation is by far the least understood. As will be described below, even basic definitions of breaking rates and incipient breaking, used in the literature, are ambiguous and often not compatible.

[4] The importance of the breaking process, however, is difficult to overestimate. The sporadic and violent breaking of waves results in major energy loss to the wave due to work done in injecting turbulence and bubbles into the upper-ocean layer. Hence, in addition to its direct impact on the wave field, breaking plays a significant role in determining the fluxes of energy, momentum and gases between the atmosphere and ocean. Therefore, breaking is also important in processes such as global weather and climate change.

[5] A detailed understanding of the breaking process has been delayed by both theoretical and experimental challenges. Intuitively, it is clear that wave steepness plays a role in wave breaking – steep waves are more prone to break. But steep waves also exhibit enhanced nonlinearity and therefore cannot be described by traditional perturbation theories where investigation of nonlinear wave properties starts from the assumption that the nonlinearity is small.

[6] Experimental investigations of breaking are very difficult due to the erratic nature of the breaking event. Although breaking waves are common on the wave surface, placing instruments in the appropriate location to investigate the breaker poses a number of logistical issues.

[7] In the present study, we initially investigate the onset of breaking using a fully nonlinear numerical model. Based on the insights provided by this model, we then investigate the physical properties of the wave which determine whether breaking will occur. These experimental investigations are performed in a laboratory wave tank, where initial conditions can be tightly controlled. This insight then enables us to suggest a parameterisation of wave breaking probability in terms of its initial monochromatic steepness (IMS) and to test our theories for open ocean data.

[8] Over the last 30 years, theoretical [e.g., *Longuet-Higgins and Cokelet*, 1978], experimental [e.g., *Melville*, 1982] and numerical [e.g., *Dold and Peregrine*, 1986] approaches have been applied to investigate instability mechanisms in nonlinear wave fields, which potentially lead to wave breaking. Although these studies have advanced the theoretical understanding of wave instabilities, there has been a clear lack of progress in our ability to predict breaking rates as a function of the physical characteristics of real wave fields and to describe these mechanisms in a form suitable for application to the continuous wave spectrum found in the field.

[9] The investigation of the properties of the incipient breaking wave is another important outcome of the present paper. The form of the incipient breaker has been predicted by analytical theories of wave breaking and is the input for practical, (i.e., engineering) applications. It is important to define, however, what is meant by an incipient breaker. Traditionally, the initial phases of a breaker-in-progress are treated as incipient breaking [e.g., *Caulliez*, 2002; *Liu and Babanin*, 2004]. Here, we suggest that the incipient breaker is defined as a wave which has already reached its limiting-stability, but has not yet started the irreversible breaking progress. This definition allows the identification of incipient breakers and, once location of the breaking onset can be predicted, measurement of the physical properties of such waves.

2. Theoretical Model and Simulations of the Onset of Breaking

[10] The numerical model employed to obtain the fully nonlinear solution of the Euler equation is the two-dimensional Chalikov-Sheinin Model (CSM) [*Chalikov and Sheinin*,

[1] Faculty of Engineering and Industrial Sciences, Swinburne University of Technology, Melbourne, Victoria, Australia.
[2] Earth System Science Interdisciplinary Center, University of Maryland, College Park, Maryland, USA.
[3] Swinburne University of Technology, Melbourne, Victoria, Australia.
[4] Rosenstiel School of Marine and Atmospheric Science, University of Miami, Miami, Florida, USA.
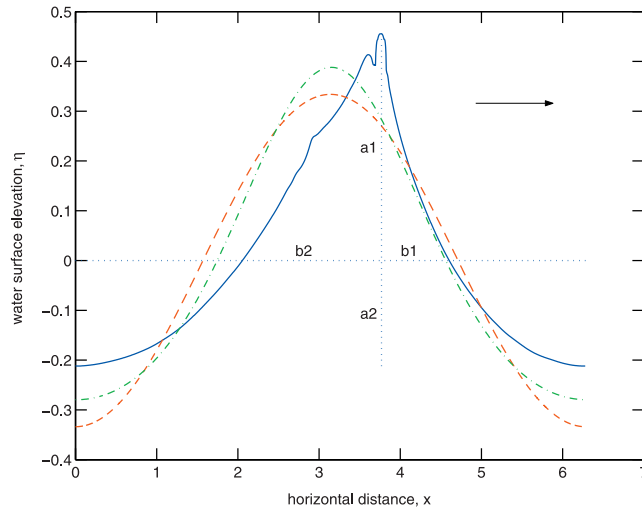
Figure 1. Three waves of different non-linearity. In all cases the waves propagate from left to right, as shown by the arrow. All three waves have the same height and wave length.

2005]. The CSM numerical approach is based on a nonstationary conformal mapping. This allows the principal equations of potential flow, with a free surface, to be written in a surface-following coordinate system. The Laplace equation retains its form, and the boundary of the flow domain, (i.e., the free surface) is the coordinate surface in the new coordinate system. Accordingly, the velocity potential over the entire domain receives a standard representation based on its Fourier expansion on the free surface. As a result, the hydrodynamic system (without any simplifications) is represented by two evolutionary equations that can provide numerical solutions, stable for many hundreds of wave periods, with very high precision [*Chalikov and Sheinin*, 2005]. Most important for this study is the model's ability to describe the evolution of very steep waves and to reproduce known strongly nonlinear features of real waves, such as wave asymmetry with respect to the vertical, which has been shown to be an inherent characteristic of wave breaking [*Caulliez*, 2002; *Young and Babanin*, 2006]. In the CSM, the wave model is coupled with an atmospheric boundary layer model. Thus, it is possible to introduce wind forcing of the waves, which tends to accelerate the breaking process.

[11] Two of the most commonly reported nonlinear features of a breaking wave are its asymmetry (i.e., the front face of the wave is steeper than the rear face) and its skewness (i.e., the crest elevation above the mean water level is greater than the trough elevation below the mean water level). Geometric definitions of skewness, S_k and asymmetry, A_s are shown in Figure 1.

[12] Following the definitions in Figure 1, the skewness and asymmetry can be defined as:

$$S_k = a_1/a_2 - 1, \qquad (1)$$

$$A_s = b_1/b_2 - 1. \qquad (2)$$

Hence, positive skewness represents a wave with a crest height greater than the trough depth and negative asymmetry represents a wave tilted forward in the direction of propagation.

[13] The incipient breaker in Figure 1 (solid line, S_k = 1.15, A_s = −0.51) was determined from the CSM by commencing the simulation with a sinusoidal (linear) wave (dashed line, S_k = 0, A_s = 0) with initial monochromatic steepness $IMS = ak = 0.25$. Here, a is the wave amplitude and k is wavenumber. Such a value of steepness is well above the limits of perturbation theory. The model is then allowed to evolve from this initial condition. It has been previously shown [*Chalikov and Sheinin*, 2005] that such a steep sinusoidal wave immediately transforms into a Stokes wave (i.e., dash-dot wave of Figure 1, S_k = 0.39, A_s = 0) whose further evolution is controlled by the Benjamin-Feir instability mechanism (BFM) [*Chalikov*, 2006]. The BFM leads to modulation of the initially monochromatic wave train, and as a result some waves can become very large at the expense of others and ultimately break.

[14] It should be pointed out that the BFM has been extensively applied to the study of the evolution of nonlinear wave groups which can lead to the breaking of a wave within the group [*Longuet-Higgins and Cokelet*, 1978; *Melville*, 1982; *Dold and Peregrine*, 1986]. The significant conceptual difference between this study and other applications of the BFM is that we do not rely on the existence of wave groups (side bands) in the initial wave field. Rather, the initial conditions consist of steep monochromatic waves and hence allow a relationship between the IMS and the onset of breaking to be developed. Side bands appear naturally and do evolve in the way described in the literature, but the cause of the side bands and therefore the key to the wave breaking rests with the IMS.

[15] In the case shown in Figure 1, $IMS = 0.25$, however, at the point of the incipient breaker shown in Figure 1 the BFM has resulted in an increase in the wave steepness to $HK/2 = 0.335$. Note that due to the nonlinear wave profile, definition of the wave steepness as ak becomes confusing (a is not now clearly defined) and hence the value $Hk/2$ has been used, where H is the wave height defined as the vertical distance between crest and trough ($H = a_1 + a_2$).

[16] Figure 2 shows the evolution of the steepness, skewness and asymmetry for an individual wave. The wave is initially sinusoidal with $IMS = 0.26$. Computations are shown for two wind forcing conditions $U/C = 2.5$ (moderate forcing) and $U/C = 5.0$ (strong forcing), where U is the wind speed and C is the phase speed of the wave with wavenumber k. Simulations cease when the water surface becomes vertical at any point (simulating breaking). In the case of the lighter wind, it takes 32 wave lengths before the wave breaks, whilst for the stronger wind this is reduced to 9 wave lengths.

[17] The most obvious features of the simulation are the oscillations in the values of steepness, asymmetry and skewness. These values oscillate at a frequency half that of the underlying wave frequency which is consistent with theoretical expectations for BFM instability [*Longuet-Higgins and Cokelet*, 1978]. The simulation begins with both skewness and asymmetry zero (sinusoidal wave). These values oscillate between their maximum and minimum values but remain bounded, their maximum and
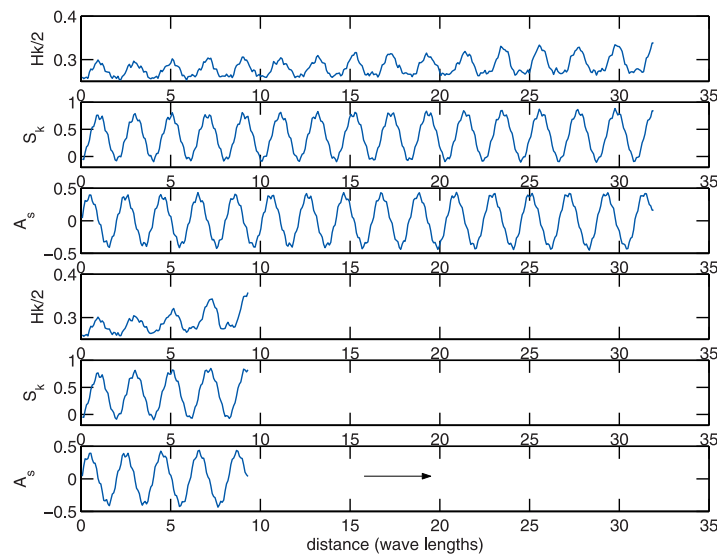
Figure 2. CSM computations of (first plot) steepness, (second plot) skewness and (third plot) asymmetry for a wave with $IMS = 0.26$. Two wind speeds are shown: top three plots, $U/C = 2.5$; bottom three plots, $U/C = 5.0$.

minimum values do not increase in magnitude. In contrast, the oscillations in the steepness progressively increase in amplitude until a point is reached where breaking takes place. It is evident from Figure 2 that it is the steepness which is the limiting parameter for breaking to occur.

[18] There is a clear phase relationship between the three quantities. The steepness and skewness are in phase, whereas the asymmetry is 90° out of phase. The wave crest increases in height, resulting in an increase in the steepness. At the point of maximal steepness and skewness, however, the asymmetry is approximately zero (i.e., wave is not tilted forward). As the peakedness decreases the asymmetry becomes negative (i.e., wave tilts forward).

[19] Further simulations demonstrated that IMS plays a critical role in determining whether or not breaking will occur. The numerical modelling showed that if $IMS > 0.3$ the wave will break immediately, within one wave length. If $IMS < 0.1$, however, the wave with no superimposed wind forcing will never break, even though it will exhibit the oscillations of steepness, asymmetry and skewness shown in Figure 2. Between these two limits, the dimensionless distance to breaking decreases with increasing IMS.

[20] The wind plays a dual role in this process. Firstly, it accelerates the growth of individual wave steepness. In the simulations shown in Figure 2, doubling the wind speed resulted in the wave growing to its critical height almost four times faster. This result is consistent with known wave growth measurements where the growth increment was shown to be a quadratic function of the wind [e.g., *Donelan et al.*, 2006]. Secondly, the wind can push the wave over and thus reduce the critical steepness, but this reduction was found to be small and only relevant at very strong wind forcing ($U/C > 10$, not shown in Figure 2).

[21] Based on the numerical simulations, it can be postulated that there is a critical steepness (IMS) above which breaking will always occur. Even if the wave is initially sinusoidal and linear, the nonlinear evolution of the wave will ultimately lead to breaking. The distance to breaking will be a function of this initial steepness. It is

these basic features which will be investigated experimentally in the following sections.

3. Experimental Investigation

[22] The experimental investigations were conducted at the Air-sea interaction tank at RSMAS, University of Miami (http://peas.rsmas.miami.edu/groups/asist). Near-monochromatic deep-water two-dimensional wave trains were generated with the wave paddle. With a tank length of 13.24 m, surface elevations were recorded at 4.55 m, 10.53 m, 11.59 m and 12.56m from the paddle. Gentle-slope beach was used to dissipate waves in the end of the tank. Surface of the slope was designed to split wave orbital velocities into multiple turbulent jets to increase viscous dissipation. Energy of reflected wave was found to be about 5–10% depending on initial wavelength. For each record, the IMS was varied in such a way that the waves would consistently break just after one of the wave probes. In this way, the dimensional distance to breaking, wave train properties immediately prior to breaking and detailed properties of the incipient breaker could be determined. The fact that breaking could be predicted and controlled by manipulating only IMS is a powerful corroboration of the numerical model.

[23] It should be pointed out that qualitative agreement between numerical model and experiment is expected, rather than an exact quantitative confirmation. Although sophisticated, the model is still a simplification of the real case and disregards contaminating features such as the natural presence of additional modes within the tank. Importantly, the two-dimensional model predicts an immediate breaking onset at $IMS > 0.3$ whereas it has been previously shown that at $ak > 0.3$ waves can exist, but a three-dimensional instability will dominate BFM [*Melville*, 1982].

[24] Figure 3 shows a wave record with an initial monochromatic frequency, $IMF = 1.8$ Hz and an $IMS = 0.30$, with no wind forcing. It should be noted that there is a conceptual change in the frame of reference compared to the
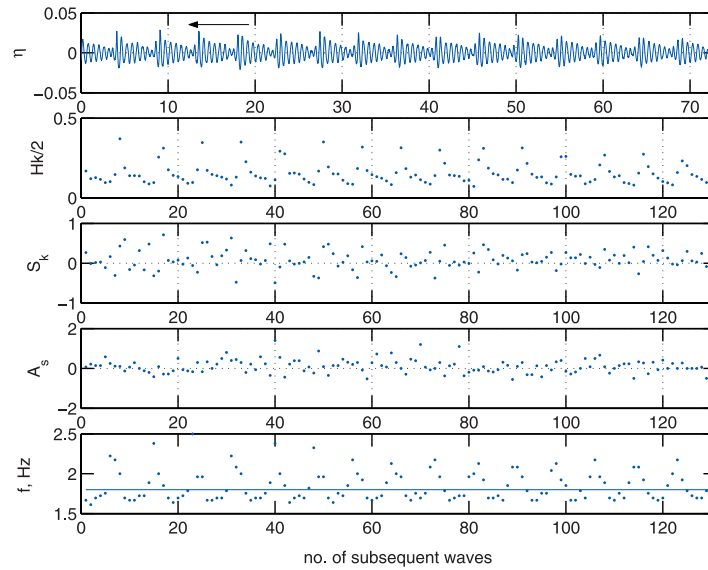
Figure 3. Segment of a time series with IMF = 1.8Hz, IMS = 0.30 and U/C = 0. The top plot shows the water surface elevation, η as a function of time in seconds. The highest wave in each group is an incipient breaker at the measurement point, breaking immediately after the wave probe. The subsequent plots show properties determined for each of the waves: (second plot) steepness, (third plot) skewness, (fourth plot) asymmetry and (bottom plot) frequency (solid line signifies IFM = 1.8Hz).

numerical model results. In the case of the model, a single wave was followed as it approached the point of breaking. Here, observations are made at a single point as a succession of waves passes. One can approximately move from the fixed frame of reference in Figure 3 to the moving frame by considering the waves shown propagating from right to left, as indicated by the arrow in Figure 3.

[25] The top plot in Figure 3 shows the measured water surface elevation (η) as a function of time (horizontal axis). Interpreting this as a wave moving from right to left shows that, within each wave group, the maximum value of the water surface elevation gradually decreases and then suddenly increases until a point, where breaking occurs. This point of breaking was located immediately after the probe at a distance of 10.73 ± 0.10 m from the wave maker. Each successive wave passing the wave gauge was analysed to determine its steepness, skewness, asymmetry and frequency, which are shown in the four plots of Figure 3.

[26] The major features seen in the numerical model are confirmed by the laboratory data. The incipient breaking waves are the steepest waves in the wave train, with the steepness oscillating in a periodic fashion. Skewness and asymmetry also oscillate, but behave in a less ordered fashion. However, at the point of breaking skewness is positive (i.e., peaked up) and asymmetry is small (i.e., not tilted forward). A feature which could not be determined from the numerical model is that there is also a modulation in the frequency. At the point of breaking the frequency increases rapidly, further increasing the steepness and hastening the onset of breaking.

[27] These visual observations are summarised in Figure 4, which shows data for the five steepest breakers. The analysis is limited to these steepest cases as wave quantities close to the breaking point change rapidly, as shown in Figure 3. These steepest cases are considered to be on the point of breaking. Like in the numerical simulations, steep-

ness seems to be the single robust criteria for breaking. For the 20 steepest breakers (not all shown in Figure 4), steepness was confined to the narrow range $Hk/2$ = 0.37 to 0.44, whilst skewness was scattered over the wide range S_k = 0 to 1 and asymmetry A_s = 0.8 to −0.4. Considering only those waves at the point of breaking, however, as in Figure 4, shows a clearer trend. The steepness appears to approach an asymptotic limit of $Hk/2 \approx 0.44$, which may represent an absolute steepness limit. We should point out that this limit is remarkably close to the theoretical steady limiting steepness of ak = 0.443 (i.e., the Stokes limit H/λ = 1/7, where $\lambda = 2\pi/k$ is the wavelength). Such an observation is very important because it signifies that the waves break once they achieve the well-established state beyond which the water surface cannot sustain its stability. It is postulated that the other geometric, kinematic and dynamic criteria of breaking, explored in the literature, are indicative of a wave approaching this state, but are not a reason or a cause for the breaking. As this limit is approached, the skewness increases very rapidly and immediately after the limit is reached the asymmetry becomes negative (i.e., the wave starts tilting forward at the point of breaking).

[28] These laboratory results are summarised in Figure 5 (top), which shows the non-dimensional distance to breaking, $N = x_b/\lambda$ as a function of IMS, where x_b is the distance to breaking. A range of values of IMS are shown, along with cases with and without wind forcing. As expected, the addition of wind forcing reduces the non-dimensional distance to breaking. However, this reduction is not so great that the data points deviate markedly from the functional relationship between N and IMS, the nonlinear effect dominating over the wind forcing.

[29] This result can be approximated by the relationship

$$N = -11 \, \text{atanh}[5.5(IMS - 0.26) + 23], \text{ for } 0.08 \leq IMS \leq 0.44.$$
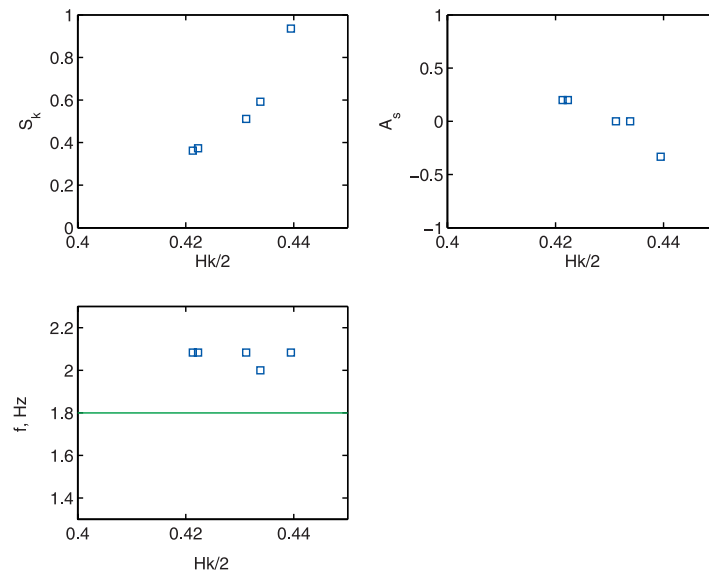(3)

Figure 4. Laboratory statistics for the incipient breakers (5 steepest waves). IMF = 1.8Hz, IMS = 0.30, U/C = 0. (top left) Skewness versus steepness. (top right) Asymmetry versus steepness. (bottom) Frequency (inverse period) versus steepness. IMF = 1.8Hz is shown with the solid line.

Consistent, with the model results, the formula imposes two threshold values of *IMS*. For *IMS* > 0.44, the wave breaks immediately (compared to *IMS* ≈ 0.3 for the two-dimensional model) and if *IMS* < 0.08 the wave, in the absence of wind forcing will never break (compared to *IMS* ≈ 0.1 for the model).

[30] In Figure 5 (top) two points (squares) are shown which were derived from Figures 1 and 2 of *Melville* [1982] for comparison. The two measurements of *Melville* [1982] were conducted for initially uniform wave trains, their initial steepness and approximate dimensionless distance to breaking being known. Although recorded under different conditions, these points agree very well with the above parameterisation and provide strong support for our results.

4. Discussion and Conclusions

[31] The relationship (3) potentially provides a means of predicting the onset of breaking in the open ocean, although some further modification is required for application to such a case. In a field situation, the notion of an initial monochromatic steepness does not exist. Besides, the waves will be three-dimensional and the mechanism which was singled out in this paper will be combined with wind forcing, current shear, superposition of dispersive spectral waves, modulation due to linear wave groups, among other relevant features. However, the above analysis suggests that should waves reach some critical steepness then they will ultimately break. It does not matter whether this limiting steepness occurred due to sustained wind forcing, wave group modulation or other means, as long as the limiting value is reached.

[32] Clearly, the breaking process is associated with individual waves, and hence a local measure of the steepness of each wave is the desired quantity. For applications (e.g., in a wave prediction model), such time-domain information is impractical and a spectral or average value

of the steepness of the wave field is the only possible quantity available.

[33] A further complication in comparing available field data with predictions of the current parameterisation is due to the fact that the relationship above predicts the probability of incipient breaking, whereas in the field it is impossible
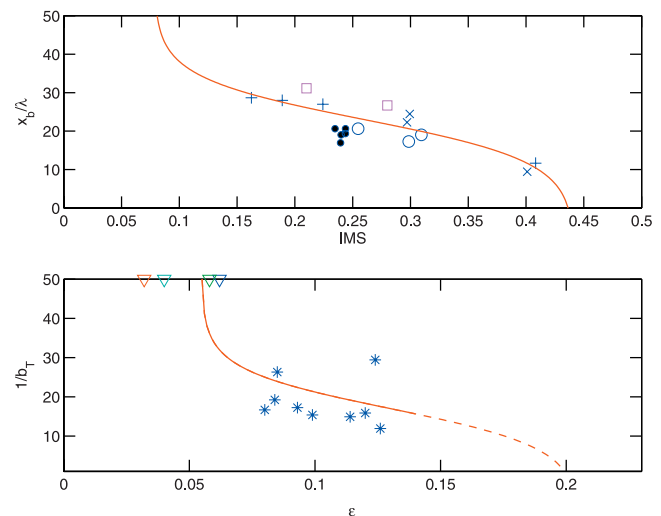

Figure 5. Parameterisation of the breaking probability. (top) Laboratory data. Number of wave lengths to breaking versus IMS. No wind forcing: o −IMF = 1.6Hz; × −IMF = 1.8Hz; + −IMF = 2.0Hz. Filled circles represent −IMF = 2.0Hz, with wind forcing applied. The parameterisation (3) is shown with solid line. (bottom) Field data. Inverse breaking probability b_T, measured by visually detected whitecaps, versus the peak spectral steepness, ε. Triangles signify measured $b_T = 0$. The line identifies the approximation (4) (the dotted part is the extrapolation based on parameterisation of *Babanin et al.* [2001]).

to directly measure whether a wave is an incipient breaker or not. At best, we can measure quantities which result from the breaking process. Common measures of this type include the acoustic signature of breaking waves or surface white-cap coverage. Although these quantities are indirect measures, they are related to the breaking process. However, a breaking wave emits an acoustic signature and forms white-caps over a substantial part of its period, and therefore the probability of encountering such sound or white-caps would be higher than the probability of breaking onset [*Liu and Babanin*, 2004].

[34] Given the uncertainties, comparison of the present parameterisation with field data can only be qualitative at this stage, as the quantities being compared are not identical. In order to conduct the comparison, the Black Sea dataset of *Babanin et al.* [2001] has been considered. Based on visual observations of white-capping, this dataset provides information on the probability of breaking, b_T of dominant waves. Dominant waves are defined in the spectral sense as frequencies near the spectral peak frequency, f_p (i.e., $f = f_p \pm 0.3f_p$). In the present context, b_T can be approximately related to N by $b_T \approx 1/N$.

[35] Figure 5 (bottom) shows $1/b_T$ as a function of the peak spectral steepness, ε, where $\varepsilon = H_p k_p/2$, $H_p = 4\left\{ \int_{0.7f_p}^{1.3f_p} F(f)df \right\}^{1/2}$, k_p is the wavenumber of the spectral peak and $F(f)$ is the frequency spectrum. An approximation to the data shown in Figure 5, consistent with the functional form of relationship (3) between N and IMS is

$$1/b_T = -10\ \text{atanh}[13.3(\varepsilon - 0.13) + 17],\ \text{for}\ 0.055 \leq \varepsilon \leq 0.205. \tag{4}$$

[36] The lower limit (no breaking if $\varepsilon < 0.055$) is obtained from the experimental data [*Babanin et al.*, 2001] and the upper limit ($\varepsilon = 0.205$) is obtained by extrapolating the parameterisation developed by *Babanin et al.* [2001] to the 100% breaking condition.

[37] Thus, we conclude that based on a combination of a nonlinear numerical model and laboratory and field data, a theory for the onset of the breaking of ocean waves has been developed and validated. Once waves reach a limiting steepness, they will ultimately break. The distance before breaking occurs is a function of the wave initial steepness.

This condition holds, even in the absence of wind forcing. The final steepness limit reached by these waves is very close to the Stokes limit, $H/\lambda = 1/7$. Benjamin-Feir instability mechanism appears to be the main hydrodynamic process which leads to achieving this limit if initial waves are steep enough. Application to field data shows that a spectral measure of wave steepness can potentially be substituted for the local steepness limit inherent in the model and laboratory data.

References

Babanin, A. V., I. R. Young, and M. L. Banner (2001), Breaking probabilities for dominant surface waves on water of finite constant depth, *J. Geophys. Res.*, *106*, 11,659–11,676.

Caulliez, G. (2002), Self-similarity of near-breaking short gravity wind waves, *Phys. Fluids*, *14*, 2917–2920.

Chalikov, D. (2006), Numerical simulation of the Benjamin-Feir instability and its consequences, *Phys. Fluids*, *19*, 016,602.

Chalikov, D., and D. Sheinin (2005), Modeling extreme waves based on equations of potential flow with a free surface, *J. Comput. Phys.*, *210*, 247–273.

Dold, J. W., and D. H. Peregrine (1986), Water-wave modulation, paper presented at 20th International Conference on Coastal Engineering, Am. Soc. of Civil Eng., Taipei.

Donelan, M. A., A. V. Babanin, I. R. Young, and M. L. Banner (2006), Wave follower measurements of the wind input spectral function. part 2. Parameterization of the wind input, *J. Phys. Oceanogr.*, *36*, 1672–1688.

Liu, P. C., and A. V. Babanin (2004), Using wavelet spectrum analysis to resolve breaking events in the wind wave time series, *Ann. Geophys.*, *22*, 3335–3345.

Longuet-Higgins, M. S., and E. D. Cokelet (1978), The deformation of steep surface waves on water. II. Growth of normal-mode instabilities, *Proc. R. Soc. London, Ser. A*, *364*, 1–28.

Melville, W. K. (1982), Instability and breaking of deep-water waves, *J. Fluid Mech.*, *115*, 165–185.

Young, I. R., and A. V. Babanin (2006), Spectral distribution of energy dissipation of wind-generated waves due to dominant wave breaking, *J. Phys. Oceanogr.*, *36*, 376–394.

————————————

A. Babanin, Faculty of Engineering and Industrial Sciences, Swinburne University of Technology, PO Box 218, Hawthorn, Melbourne, Vic 3122, Australia. (ababanin@swin.edu.au)

D. Chalikov, Earth System Science Interdisciplinary Center, University of Maryland, 3439 Comp. and Space Sci. Bldg., College Park, MD 20742-2465, USA.

I. Savelyev, Rosenstiel School of Marine and Atmospheric Science, University of Miami, 4600 Rickenbacker Causeway, Miami, FL 33149-1098, USA.

I. Young, Swinburne University of Technology, Hawthorn, Melbourne, Vic 3122, Australia.